ELSEVIER

Cement & Concrete Composites 26 (2004) 453–461

Cement & Concrete Composites

www.elsevier.com/locate/cemconcomp

A unified solidification model of hardening concrete composite for predicting the young age behavior of concrete

R. Mabrouk *, T. Ishida, K. Maekawa

Department of Civil Engineering, The University of Tokyo, Hongo 7-3-1, Bunkyo-ku, Tokyo 113-8556, Japan

Abstract

The prediction of hardening young concrete behaviors is proposed using a solidification model based on the microphysical information of temperature, hydration ratio, porosity, saturation, isotherm and others. The solid model deals with cement paste as the solidified finite fictitious clusters having each creep property. Aggregates are idealized as suspended continuum media of perfect elasticity. The combination of both phases may create the overall features of concrete composite under the unstable transient conditions at early age. The micro-scale surface tension is treated as the driving force for the shrinkage associated with and without water migration. The solidification model is expected to offer the deformability of hardening concrete under the combined effect of external loads and the capillary stress estimated by the thermo-dynamic computation. Verification of the proposed model is conducted through comparison with some experimental data available in the literature.

Keywords: Young age concrete; Shrinkage; Creep; Multiphase material; Microphysics; Solidification; Constitutive modeling; Elasticity; Plasticity; Viscosity

1. Introduction

The early stage of concrete life is known to have a significant control on the overall performance of concrete structures. In fact, it can be said that the future of a reinforced concrete structure may be decided based upon the information obtained from this period.

Due to this, several models dealing with concrete at the early age have been proposed. These models can generally be divided into two groups. The first uses a parameter such as maturity [1] or degree of hydration [2] to represent the aging process. While the other group is based on some form of curve fitting using the mathematical formulation of Maxwell or Kelvin chains [3]. The aforementioned models have many shortcomings and could only give a narrow range of predictability. Recently, some models that are based on the assumptive physical phenomena in concrete such as moisture transport or microstructure of cement paste are being studied. These types of models show a better understanding of the young concrete behavior and thus are better suited for establishing more reasonable formulations. Some of the models that have shown good potential are the solidification theory [4], the model by Anders Boe Hauggaard-Nielsen [5,6] and the Lokhorst creep estimation model [7,8]. In this research, a model based on the solidification theory will be proposed.

2. Basic concept of the proposed model

The basic concept of this method is to predict the behavior of concrete based on the actual thermo-hygro-physical information of the microstructure. The input data is the concrete information like mix proportions, type of cement and environmental conditions of temperature and relative humidity, structure information like size, shape, reinforcement and loading conditions. Microphysical information of temperature, hydration ratio, pore structure and moisture transport are calculated using the computational framework DuCOM [9,10]. Where, a dynamic coupling of cement hydration, microstructure formation and moisture transport models is incorporated. This information is then also used as input data in the proposed model. This input data of microphysical information are linked to the structural

* Corresponding author. Tel.: +81-3-5841-7498; fax: +81-3-5841-6010.

E-mail address: rasha@concrete.t.u-tokyo.ac.jp (R. Mabrouk).

0958-9465/$ - see front matter © 2003 Elsevier Ltd. All rights reserved.
doi:10.1016/S0958-9465(03)00073-8

behavior of concrete. For instance, the stiffness and strength are related to the microstructure development. The volumetric change provoked by the hydration in progress and water loss is physically linked to the surface tension force developing inside the micro-capillary pores. The creep deformation is correlated with the moisture movement and the microstructure of the cement paste.

The various performances of concrete like autogenous shrinkage, drying shrinkage, basic creep, drying creep and thermal deformations are considered. One advantage and innovative property of this research is that it attempts to deal with these behaviors using only one microphysical model in a unified manner without any separation of creep and shrinkage. In addition, contrary to most of the current empirical models, the proposed solidification model can deal with the minute prediction involving structural detail and time dependent variation in environmental conditions as well as the evaluation of stress distribution within the different locations of the structure. The first version of the model was previously proposed [11]. Currently, a more comprehensive and general proposal is introduced which attempts to cover the behavior of concrete not only at the early age but also the behavior of mature concrete as well.

3. Mathematical model

It is convenient in material modeling to decompose the stress tensor into two parts; the volumetric tensor and the deviatoric tensor. The same procedure will be applied here. The volumetric stress tensor is the tensor whose elements are $\sigma_0\delta_{ij}$ where σ_0 is the mean volumetric stress and δ_{ij} is the Kronecker delta function. The mean volumetric stress is given by Eq. (1). The deviatoric stress tensor is thus obtained by subtracting the volumetric stress tensor from the total stress as shown in Eq. (3). The same procedure can be applied to the strain tensor as shown in Eqs. (2) and (4):

$$\sigma_0 = \tfrac{1}{3}(\sigma_{xx} + \sigma_{yy} + \sigma_{zz}) = \tfrac{1}{3}I_1 \tag{1}$$

$$\varepsilon_0 = \tfrac{1}{3}(\varepsilon_{xx} + \varepsilon_{yy} + \varepsilon_{zz}) \tag{2}$$

$$S_{ij} = \sigma_{ij} - \sigma_0\delta_{ij} \tag{3}$$

$$e_{ij} = \varepsilon_{ij} - \varepsilon_0\delta_{ij} \tag{4}$$

where, I_1 is the first invariant of stress tensor, S_{ij} is the deviatoric stress tensor and σ_{ij} is the total stress tensor. ε_0 is the mean volumetric strain, e_{ij} is the deviatoric strain tensor and ε_{ij} is the total strain tensor.

3.1. Volumetric component

In this study, concrete is treated as a two-phase solid dispersion system, namely aggregate and cement paste (Fig. 1). Concerning the coupling of aggregate and cement paste, virtual work principle can be utilized for theoretically deriving the mean stress and strain on the aggregate and cement paste. Hence, the volumetric invariant for the two-phase system can be defined with respect to the component ones as shown in Eqs. (5) and (6). In addition to these two equations, the two constitutive laws for each component of aggregate and cement paste can also be used. Aggregate is assumed as linear elastic as shown in Eq. (7). Eq. (8) represents the constitutive relation for cement paste, which will be discussed in details in Sections 3.3–3.7:

$$\overline{\sigma}_0 = \rho_{ag}\overline{\sigma}_{ag} + \rho_{cp}\overline{\sigma}_{cp} \tag{5}$$

$$\overline{\varepsilon}_0 = \rho_{ag}\overline{\varepsilon}_{ag} + \rho_{cp}\overline{\varepsilon}_{cp} \tag{6}$$

$$\overline{\varepsilon}_{ag} = \frac{1}{3K_{ag}}\overline{\sigma}_{ag} \tag{7}$$

$$\overline{\varepsilon}_{cp} = f(\overline{\sigma}_{cp}) \tag{8}$$

where, $\overline{\sigma}_0$, $\overline{\sigma}_{ag}$ and $\overline{\sigma}_{cp}$ are the mean volumetric stresses on concrete, aggregate and cement paste, respectively, and $\overline{\varepsilon}_0$, $\overline{\varepsilon}_{ag}$ and $\overline{\varepsilon}_{cp}$ are the mean volumetric strains, ρ_{ag} and ρ_{cp} are the volume fractions of aggregate and cement paste, respectively. K_{ag} is the volumetric stiffness of aggregate.

In addition to the above, one more equation based on the shear rigidity of cement paste is introduced. It may be assumed that the composite of aggregate and cement paste can be represented by a combination of Maxwell and Kelvin chains of viscous continuum. If the cement paste matrix would be a perfect liquid losing resistance to the shear deformation, then, $\overline{\sigma}_{ag} = \overline{\sigma}_{cp}$, where, the

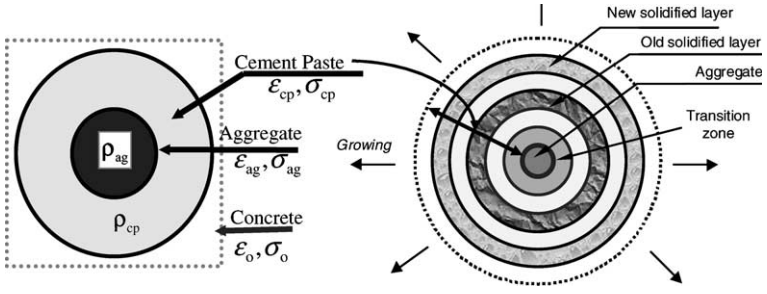

Fig. 1. Schematic representation of aggregate, cement paste and the solidification process.

shear stiffness of cement paste becomes zero. This system corresponds to a Maxwell chain. On the contrary, if the shear stiffness, G_{cp}, is infinitely large, it brings no shear deformation at all, and the deformed shape with volumetric expansion or contraction is perfectly similar to the referential shape at an initial time. Thus, $\overline{\varepsilon}_{ag} = \overline{\varepsilon}_{cp}$. This system corresponds to a Kelvin chain. The actual case is somehow in between these two cases. One of the possible formulas is the Lagragian method of linear summation as shown by Eq. (9):

$$\left(\frac{\overline{\sigma}_{ag} - \overline{\sigma}_{cp}}{G_{cp}}\right) + (\overline{\varepsilon}_{ag} - \overline{\varepsilon}_{cp}) = 0 \tag{9}$$

3.2. Deviatoric component

The same procedure used for volumetric component can be applied here. However, for simplicity and assuming free rotation of the suspended particles, the shear component of the aggregate phase can be neglected. Therefore the shear strains and stresses of concrete are equal to that of the cement paste. In this case, the system is reduced to one equation, which is the constitutive relation for cement paste as shown in Eq. (10):

$$S_{ij} = f(e_{ij}) \tag{10}$$

where, (S_{ij}) and (e_{ij}) are the deviatoric stress tensor and the deviatoric strain tensor for cement paste, respectively such that $S_{ij} = [S_{xx}\ S_{yy}\ S_{zz}\ S_{xy}\ S_{yz}\ S_{zx}]^{T}$ and $e_{ij} = [e_{xx}\ e_{yy}\ e_{zz}\ e_{xy}\ e_{yz}\ e_{zx}]^{T}$.

3.3. Constitutive formulation for cement paste

The structure growth of cement paste is a rather complex procedure. Upon contact with water, the powder particles start to dissolve and the reaction products start to form. Due to the gradual solidification of the hydration products the properties of the paste vary considerably with time. As mentioned before, the solidification theory [4] proved a potential way of taking this aging effect into consideration and thus it will be utilized in this research.

As shown in Fig. 1, the growth of cement paste is idealized by the formation of finite fictitious clusters or layers. This means that after a new layer is formed, its properties do not change with time but the aging process itself is represented by the solidification of new layers. In order to set a criterion for the layer formation a volume fraction function is introduced. This function is taken as the hydration ratio at a certain time t, $\psi(t)$. It is defined as the ratio of the hydrated volume of cement powder, $V(t)$, to the total volume of cement that is available for hydration, V_{cp}, as shown by Eq. (11):

$$\psi(t) = V(t)/V_{cp} \tag{11}$$

The structure of the cement paste at any time is represented using the number of the layers already solidified at that time. According to the value of the hydration degree, the number of layers, N, at a certain time can be determined and when the hydration increment reaches a certain value a new layer is developed and attached to the older ones. These layers share in bearing the stresses carried by the cement paste, thus, introducing an infinitesimal stress in each layer, S_{cp}. When a new layer is formed, these infinitesimal stresses are redistributed among the layers. This also means that the stress condition in a certain layer is a function of both the current time and the location of this layer or the time when this layer solidified. Thus, if S_{cp} denotes the average stress in a general layer, t is the time and t' is the time when this layer is solidified. Then, it can be stated that, $S_{cp} = S_{cp}(t, t')$.

3.4. Coupling of the system of cement paste layers

Concerning the coupling of the system of fictitious layers, they are assumed to join forming a parallel system. Thus, the total volumetric stress in cement paste at a certain time is the summation of the average stresses in all individual layers found at that time and the strain in cement paste is equal to the strain induced in each layer. Fig. 2 shows the correlation between the solidification of cement paste layers and the growth of the microstructure. Eq. (12) gives the total stresses in the cement paste for the volumetric part. For the deviatoric part, each of the six components of the stress tensor S_{ij} is equal to the summation of the corresponding components over all layers found at time, t, as can be shown using Eq. (13):

$$\overline{\sigma}_{cp}(t) = \int_{t'=0}^{t} S_{cp}(t', t)\, d\psi(t') \tag{12}$$

$$S_{ij}(t) = \int_{t'=0}^{t} S_{ij}(t', t)\, d\psi(t') \tag{13}$$

where, $\overline{\sigma}_{cp}(t)$ is the mean volumetric stress on cement paste, $S_{cp}(t', t)$ is the mean volumetric stress acting on a certain layer, t' is the time when this layer solidified, t is the current time, ψ is the hydration degree, $S_{ij}(t)$ is the deviatoric stress tensor acting on cement paste and $S_{ij}(t', t)$ is the deviatoric stress tensor acting on a certain layer.

It should be noted here that when a new layer is just formed it should be stress free. That is because this layer would be in contact with the unhydrated cement and water in a liquid state and it would be physically incorrect to assume that such a layer could solidify in a stressed state. Thus we have, $S_{cp}(t, t) = 0$ and $S_{ij}(t, t) = 0$.

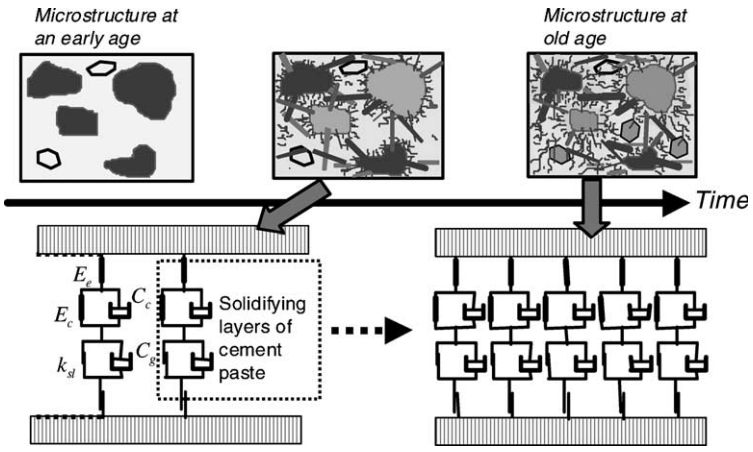

Fig. 2. Solidifying layers of cement paste and aging of the microstructure.

3.5. Modeling for individual layers of cement paste

In the previous sections, the general system of layers, representing the growth of the cement paste, and their coupling has been explained. Now, the modeling of each of these fictitious non-aging layers needs to be discussed. In this research, it will be assumed that creep occurs as a result of the moisture transport through the different pores of the microstructure. The size and range of these pores are distributed over a wide range. These can be divided into the following categories [9,10]:

- Capillary pores: which are empty spaces left between the partially hydrated cement grains.
- Gel pores: which are formed as an internal geometrical structure of the CSH grains.
- Interlayer pores: which are considered as a structural part of the CSH grains.

Moisture transport actually takes place into the capillary and gel pores. However, under severe conditions motion of interlayer water could be observed. It can be assumed that moisture transport related to each of these pores categories can be correlated to a certain aspect of the creep behavior [12,13]. This can be explained as follows.

The rate of flow of capillary water is comparatively high and can easily be reversible. Thus, moisture transport within the capillary pores can be assumed as the cause of the short-term creep or creep at the earlier age. This creep rate drops steeply with time and is highly related to the hydration process. Moisture transport within the gel pores is somehow slow and prolonged. This motion of the gel water can be reversible up to a certain limit. It can be assumed as the cause of the long-term creep and is responsible for the main part of the residual creep. Moisture transport within interlayer pores can be assumed as the cause of creep under severe conditions. This creep is highly irreversible.

In order to reflect the three aspects of creep behavior mentioned above, the rheological model for each layer is assumed as shown in Fig. 3. The same model is adopted for both the volumetric and the deviatoric components. Here, the volumetric component is discussed in details. However, the same procedure is conducted for each of the six components of the deviatoric part. In this model, the total strain is decomposed into instantaneous elastic strain; ε_e, visco-elastic strain; ε_c, visco-plastic strain; ε_g and viscous strain; ε_l:

$$\varepsilon'_{cp} = \varepsilon_e + \varepsilon_c + \varepsilon_g + \varepsilon_l \tag{14}$$

where ε'_{cp} is the volumetric strain in a general layer.

It should be noted here that $\overline{\varepsilon}'_{cp}(t)$ is the strain induced in a certain layer after its solidification. As the layers are assumed to join in parallel, then these strains should be equal to the corresponding volumetric strain in cement paste. However, the layers solidify at zero stress state. Therefore, as shown in Eq. (15), this strain at a certain time, t, is defined as the difference between the strain of cement paste at time, t, and the strain of cement paste at the time when the layer solidified, t':

$$\overline{\varepsilon}'_{cp}(t) = \overline{\varepsilon}_{cp}(t) - \overline{\varepsilon}_{cp}(t') \tag{15}$$

3.6. Elements of the rheological model for each layer

3.6.1. Elastic part

Represented using a perfectly elastic spring:

$$S_{cp} = E_e \cdot \varepsilon_e \tag{16}$$

where, S_{cp} is the volumetric stress in a general layer, E_e is the stiffness of the elastic spring and ε_e is the instantaneous elastic strain. The elastic stiffness, E_e, is calculated such that the summation of stiffness over all layers at a certain time is equal to that of cement paste at this time.

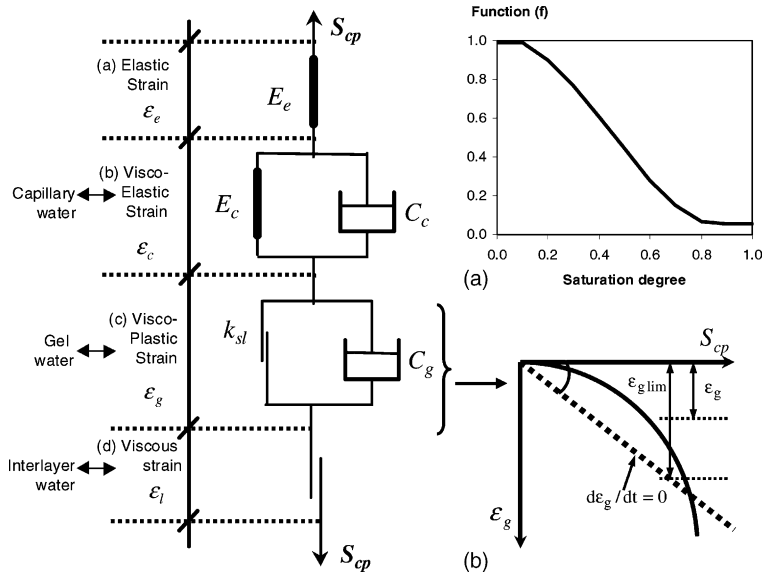

Fig. 3. Rheological model for each layer of cement paste: (a) variation of the dash pot constants against saturation degree and (b) visco-plastic component formulation.

3.6.2. Visco-elastic part

Represented using a Kelvin-chain of an elastic spring and a dashpot. It is mainly related to the motion of water in the capillary pores:

$$S_{\mathrm{cp}} = E_{\mathrm{c}} \cdot \varepsilon_{\mathrm{c}} + C_{\mathrm{c}} \frac{\mathrm{d}\varepsilon_{\mathrm{c}}}{\mathrm{d}t} \tag{17}$$

where, E_{c} is the stiffness of the elastic spring and is assumed as $2.0E_{\mathrm{e}}$. ε_{c} is the visco-elastic strain. C_{c} is the constant of the dashpot fluid.

The constant of the dashpot, C_{c}, is related to the water motion through the capillary pores associated with thermo-hygro-physical requirements. Thus, the dashpot constant for an arbitrary layer can be obtained from Eq. (18) as follows:

$$C_{\mathrm{c}} = a \cdot f(S_{\mathrm{cap}}) \cdot \eta^{b} \cdot \phi_{\mathrm{cap}}^{c} \tag{18}$$

where, a is a constant, ϕ_{cap} is the capillary porosity of the paste, S_{cap} is the saturation of the capillary pores, η is the viscosity of the water in the micropores and b and c are constants taken as 1 and -1, respectively. Function, f, can be defined as shown in Fig. 3(a).

3.6.3. Visco-plastic part

This part is assumed to be totally irreversible as it is mainly related to the motion of water from the gel pores. To simulate this, it is represented using a one way slider and a dashpot. For simplicity in mathematical formulation, Eq. (19) is used. Here it is assumed that the limiting value of the visco-plastic strain, where the rate of strain becomes zero, is represented as a function of the stress acting on the layer as shown in Fig. 3(b). This function is simplified using a linear relation as shown in Eq. (19). The limiting value of gel strain $\varepsilon_{\mathrm{glim}}$ is assumed not only as a function of the acting stress but also as a function of the saturation level of the gel pores. When the gel pores are filled with water, the strain rate is very slow even if a high value of stress is applied. On the contrary if the gel pores are empty, when stress is applied a high strain rate can be observed:

$$\varepsilon_{\mathrm{glim}} = f_1(S_{\mathrm{cp}}) \cdot f_2(S_{\mathrm{gel}}) \tag{19}$$

where, S_{gel} is the saturation of the gel pores and S_{cp} is the volumetric stress of the layer.

$f_1(S_{\mathrm{cp}})$ = the limiting value of visco-plastic strain if $S_{\mathrm{gel}} = 0.0$

$f_1(S_{\mathrm{cp}}) = S_{\mathrm{cp}}/E_{\mathrm{g}}$ and $E_{\mathrm{g}} = E_{\mathrm{e}}/4.0$

$f_2(S_{\mathrm{gel}}) = e^{-aS_{\mathrm{gel}}}$ and a is a constant.

The rate of gel strain can then be computed using Eq. (20):

$$\frac{\mathrm{d}\varepsilon_{\mathrm{g}}}{\mathrm{d}t} = Q(\varepsilon_{\mathrm{glim}} - \varepsilon_{\mathrm{g}}) = k(\varepsilon_{\mathrm{glim}} - \varepsilon_{\mathrm{g}}) \tag{20}$$

where, ε_{g} is the visco-plastic strain and $\varepsilon_{\mathrm{glim}}$ is its limiting value. Q is assumed as a linear function such that $k = 1.0/C_{\mathrm{g}}$. C_{g} can be obtained as follows:

$$C_{\mathrm{g}} = d \cdot f(S_{\mathrm{gel}}) \cdot \eta^{b} \cdot \phi_{\mathrm{gel}}^{c} \tag{21}$$

where d is a constant, ϕ_{gel} is the gel porosity of the paste related to this arbitrary layer, S_{gel} is the saturation of the gel pores, η is the viscosity of the water in the micropores and b and c are constants taken as 1.

3.6.4. Viscous part

Represented using a slider. It is mainly related to the motion of water through the interlayer pores:

$$\Delta\varepsilon_{\mathrm{l}} = z \cdot \Delta S_{\mathrm{int}} \tag{22}$$

where ε_{l} is the viscous strain, z is a constant and S_{int} is the saturation of the interlayer.

The above Eqs. (14)–(22) are solved together so that finally a relation between the stress and strain of the cement paste layer can be obtained.

3.7. Coupling of skeleton stresses and pore water pressure

Many theories have been proposed describing the mechanism of drying shrinkage in concrete. In this research, the most generally used capillary tension theory is adopted where the tensile stress induced on the cement paste due to the pressure difference between the liquid phase and the gas phase is assumed as the cause of the shrinkage deformation [14].

Thus, the combined effect of external loads and pore water pressure created by the micro-scale surface tension is treated as the driving force for the deformation of the cement paste. Accordingly, the total average volumetric stress on cement paste $\overline{\sigma}_{\mathrm{cp}}$ is calculated by using Eqs. (23) and (24). The total intensity of the tensile stress per unit paste volume will depend on both the magnitude of the tension and the area where it is applied [9,10,14]. Therefore, the factor β is introduced which is related to the actual amount of liquid water per unit paste volume (Eq. (25)):

$$\overline{\sigma}_{\mathrm{cp}} = \overline{\sigma'_{\mathrm{cp}}} + \beta \cdot \sigma_{\mathrm{s}} \tag{23}$$

$$\sigma_{\mathrm{s}} = -\frac{2 \cdot \gamma}{r_{\mathrm{s}}} = -\frac{\rho \cdot R \cdot T}{\mathrm{M}} \ln h \tag{24}$$

$$\beta = \frac{\phi_{\mathrm{cap}} \cdot S_{\mathrm{cap}} + \phi_{\mathrm{gel}} \cdot S_{\mathrm{gel}}}{\phi_{\mathrm{cap}} + \phi_{\mathrm{gel}}} \tag{25}$$

where $\overline{\sigma}'_{\mathrm{cp}}$ is the mechanical stress carried by the skeleton of cement paste, σ_{s} denotes the tensile stress due to the pressure difference calculated by the thermo-hygro-physical approach. γ is the surface tension of liquid water and r_{s} is the pore radius at which the interface is created. R is the universal gas constant, T is the absolute temperature of the vapor–liquid system, M is molecular

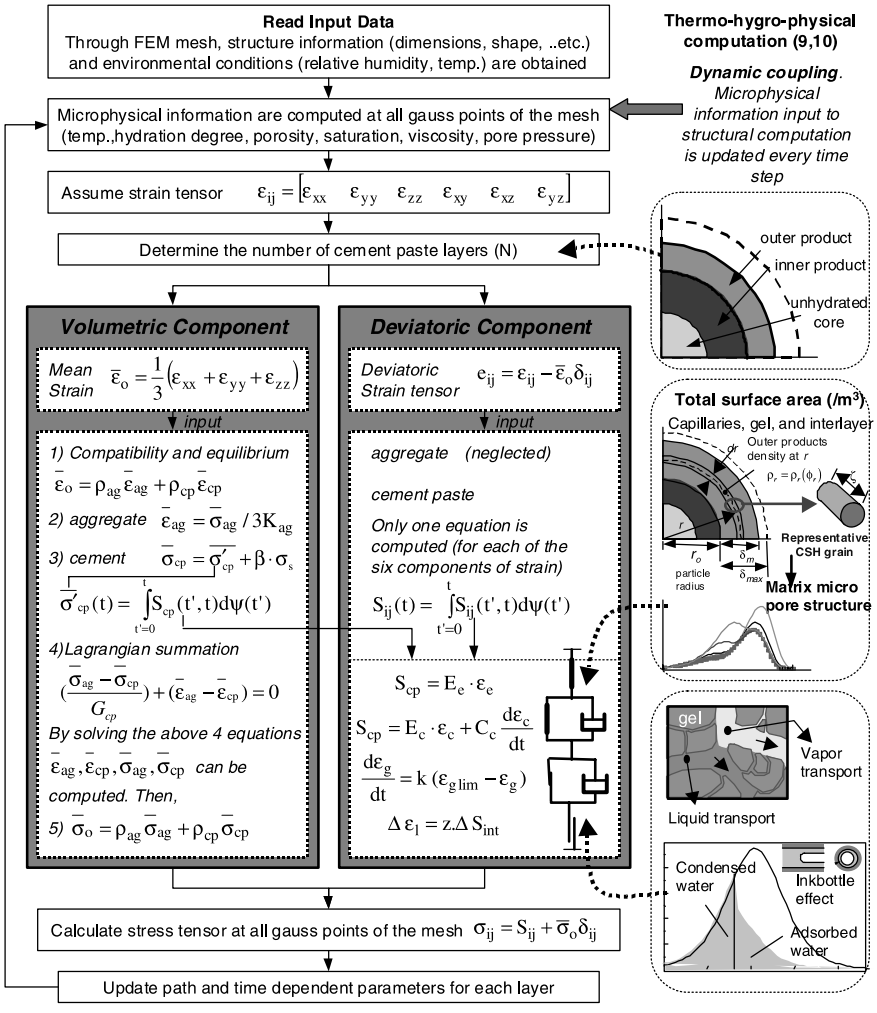

Fig. 4. Flow chart for the model computation and the coupling with thermo-hygro-physics.

mass of the water and h is the relative humidity i.e. the ratio of the vapor pressure to the saturated vapor pressure. ϕ_{cap} and ϕ_{gel} are the porosity of capillary and gel, respectively. S_{cap} and S_{gel} are the saturation of capillary and gel, respectively.

4. Verification of the proposed model

In this section, the framework involving both the computation of thermo-hygro-physical information and the simulation of the structure behavior is presented. Fig. 4 shows the outline of the computation scheme and the coupling with the thermo-hygro-physical mechanisms used. Fig. 5 shows a summary of the model parameters and their computation. The finite elements analysis program DuCOM [9,10], that has been developed at The University of Tokyo, is used. In the next section, verification of the major components of the model is attempted. An analytical study of creep and shrinkage was done using the proposed model and comparison with available experimental data was conducted. The data of the studied specimens is shown in Table 1.

Firstly, two pure cement paste specimens were studied, S1 and S2. These specimens are a part of a group of tests conducted at Concrete Laboratory at the University of Tokyo. The results are shown in Fig. 6. These two cases can be used to study the system computation at young age as a whole. Here, the aging process represented by the solidification of layers, creep at young age as represented by the visco-elastic part and the coupling

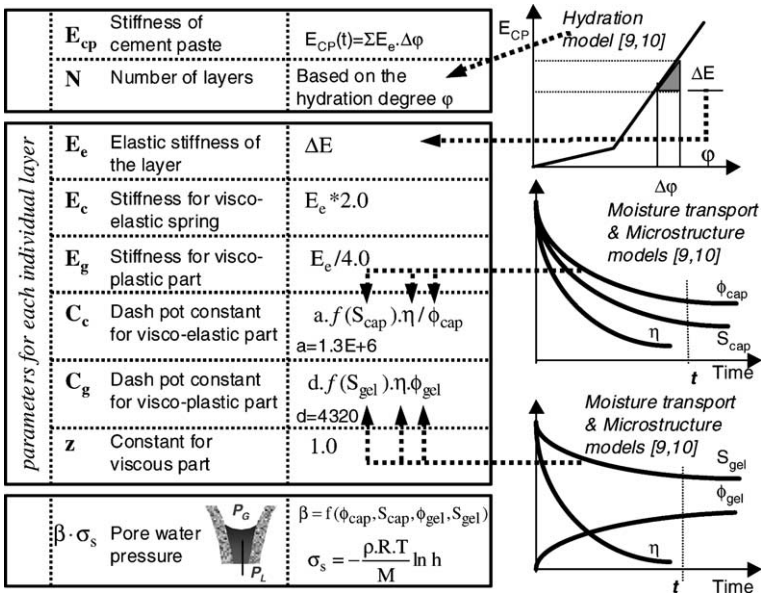

Fig. 5. Summary of the model parameters and their computation.

Table 1
Date of the specimens used in the verification of the model

	Size (cm)	W/C[a] (%)	V_{agg}[b] (%)	Type of cement	RH[c] (%)	Age at drying (days)	Load	Age at loading/unloading (days)
S1	Cyl. 10 × 20	30	Zero	OPC[d]	80	1	–	–
S2	Cyl. 10 × 20	30	Zero	OPC[d]	80	1	5 MPa	1/2/3/4/7
S3 [15]	10 × 10 × 120	28	62	OPC[d]	50	1	–	–
S4 [16]	Cyl. 5 × 20	40	62	OPC[d]	32	1	10 MPa	28/108
S5 [16]	Cyl. 5 × 20	40	62	OPC[d]	95	1	15 MPa	28/148
S6 [17]	Beam 2.27 × 2.27 × 83.5	32	Zero	OPC[d]	Sealed	–	40 N (applied at mid span)	28
S7 [17]	Beam 2.27 × 2.27 × 83.5	32	Zero	OPC[d]	Sealed	–	40 N (applied at mid span)	28

[a] W/C = the water to cement ratio.
[b] V_{agg} = the ratio of aggregate in the mix by volume.
[c] RH = the environmental relative humidity.
[d] OPC = Ordinary Portland Cement.

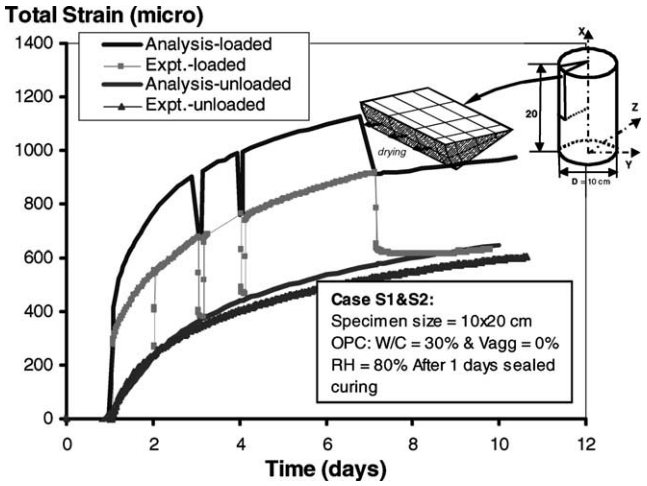

Fig. 6. Comparison between experimental and analytical results for case S1 and S2.

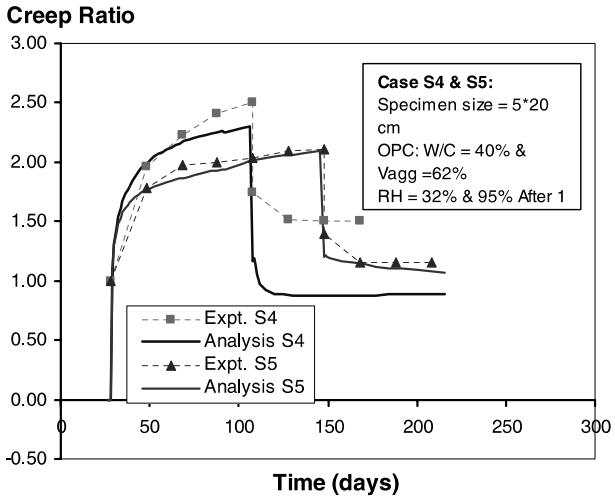

Fig. 8. Comparison between experimental and analytical results for cases S4 and S5.

with the pore water pressure for computation of shrinkage are the main parts affecting the results. From the figure, good agreement can be obtained between the analysis and experiment in case of drying shrinkage, S1, while the results are rather overestimated in the case of loaded specimen, S2.

In the following cases, verification of separate phenomena is attempted. Fig. 7 shows the results of a case of drying shrinkage of concrete, S3 [15]. Reasonable agreement can be obtained between experimental and analytical results. This case verifies the coupling between the skeleton stress of cement paste and the pore water pressure.

In Fig. 8, two concrete cylinder specimens were studied S4 [16] and S5 [16]. The results shown are the values of creep ratio, which is the creep strain per unit stress. Case S5 shows that of creep under sealed conditions at the age of 28 days. In this case the effect of drying is not existing and the aging process is almost completed. The main factor in computation would be that of the cement paste springs. In case of S4, drying is allowed. Therefore, here the effect of the visco-plastic component becomes more apparent and the creep values are increased. Comparison between experiment and analysis are quite reasonable. However, the irreversible part in case of drying is rather underestimated.

In addition to the above, two cement paste beams were studied S6 [17] and S7 [17]. The analytical and experimental results are shown in Figs. 9 and 10. These two cases represent a simple verification on the structure level. Once again reasonable results can be obtained. It can also be shown that the loading–unloading pattern in case of S7 can be well represented. This part is mainly linked to the slider and dashpot of the visco-plastic component.

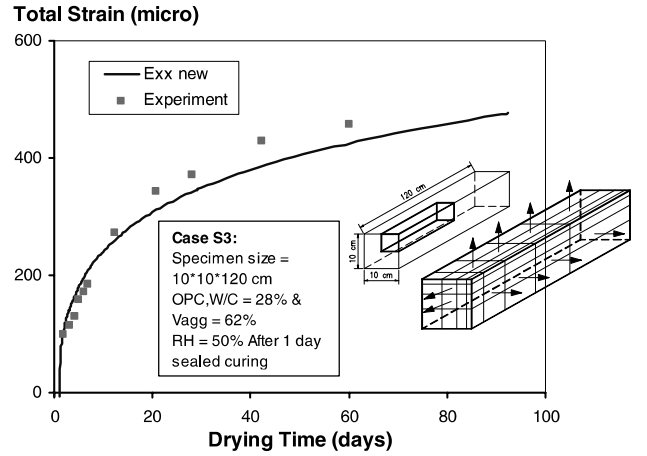

Fig. 7. Comparison between experimental and analytical results for case S3.

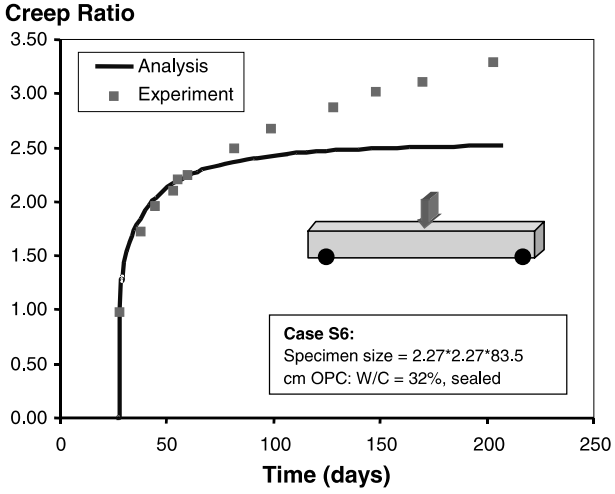

Fig. 9. Comparison between experimental and analytical results for case S6.

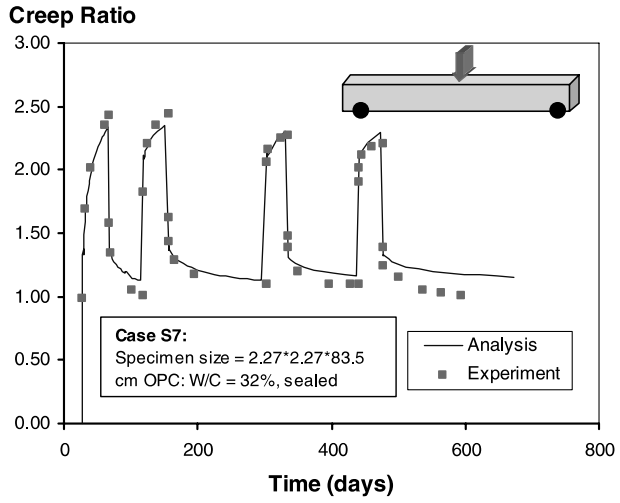

Fig. 10. Comparison between experimental and analytical results for case S7.

5. Conclusions

In this analysis, the modeling of the behavior of the hardening concrete composite is attempted using a solidification model based on the microphysical information of temperature, hydration ratio, porosity, saturation, isotherm and others. Through this coupling between constitutive modeling and microphysical information, the behavior of young age concrete composite can be rationally predicted.

Comparison with some experimental data form the literature proved that the proposed model shows reasonable agreement with experiments. Different cases were studied having various conditions of loading and environmental conditions and in most cases reasonable results were obtained. There are many phenomena to be checked using the proposed model and many mechanisms are involved in computation. Extensive verifications and modifications are still needed. However, it could be shown that this framework can be a solid method for the determination of behavior of concrete under variable conditions. It also shows that the model not only represent concrete at the young age, but also can be extended to simulate old age concrete. With some enhancement of the model parameters this model shows good future prospects.

References

[1] Carino NJ. The maturity method: Theory and application. Cement Concrete Aggr 1984;6(2):61–73.
[2] Breugel K. Numerical modeling of volume changes at early ages—potential, pitfalls and challenges. Mater Struct 2001;34:293–301.
[3] Neville AM. Creep of concrete: plain, reinforced and prestressed. Amsterdam: North-Holland Publishing Company; 1970.
[4] Bazant ZP, Prasannan S. Solidification theory for concrete creep. I. Formulation, II. Verification and application. J Engng Mech 1989;115(8):1691–725.
[5] Bazant ZP, Hauggaard AB, Baweja S. Microprestress solidification theory for aging and drying creep of concrete. Advances in Building Materials Science, Festschrift Prof. Wittmann. AEDIFICATIO Publishers. p. 111–30.
[6] Hauggaard-Nielsen, AB. Mathematical modeling and experimental analysis of early age concrete. Report of University of Denmark, 1997.
[7] Lokhorst SJ, Breugel K. Simulation of the effect of geometrical changes of the microstructure on the deformational behavior of hardening concrete. Cement Concrete Res 1997;27(10):1465–79.
[8] Lokhorst SJ. Deformational behavior of concrete influenced by hydration related changes of the microstructure. TU Delft internal report, 1995.
[9] Maekawa K, Chaube R, Kishi T. Modeling of concrete performance. London: E & FN SPON; 1999.
[10] Maekawa K, Ishida T. Service-life evaluation of reinforced concrete undercoupled forces and environmental actions. Materials Science of Concrete, special volume, Ion and mass transport in cement-based materials 2001:219–38.
[11] Mabrouk R. Unified constitutive law of solidifying concrete composite and application to reinforced concrete structures. PhD thesis. Tokyo, The University of Tokyo, 1999.
[12] Neville AM. Theories of creep in concrete. J Am Concrete Inst 1955;52(1):47–60.
[13] Glucklich J, Ishai O. Creep mechanism in cement mortar. J Am Concrete Inst 1962;59(34):923–47.
[14] Shimomura T, Maekawa K. Analysis of the drying shrinkage behavior of concrete using a micromechanical model based on the micropore structure of concrete. Mag Concrete Res 1997;49(181):303–22.
[15] Kato, T. Shrinkage and deformation property of concrete structure under drying conditions. Master thesis submitted to the University of Tokyo, 1997.
[16] Neville AM. Creep recovery of mortars made with different cements. J Am Concrete Inst 1959;56(13):167–74.
[17] Glucklich J. Rheological behavior of hardened cement paste under low stress. J Am Concrete Inst 1959;56(23):327–37.